ELSEVIER

Journal of Chromatography A, 918 (2001) 37–46

JOURNAL OF CHROMATOGRAPHY A

www.elsevier.com/locate/chroma

Contribution of axial dispersion to band spreading in perfusion chromatography

Anli Geng, Kai-Chee Loh*

Department of Chemical and Environmental Engineering, National University of Singapore, 10 Kent Ridge Crescent, Singapore 119260, Singapore

Received 7 September 2000; received in revised form 16 January 2001; accepted 28 February 2001

Abstract

A new interpretation of the band spreading data in perfusion chromatography is proposed by investigating the relative importance of axial dispersion in perfusive beds. Elution chromatography of proteins (bovine serum albumin and lysozyme) under non-retained conditions on two kinds of reversed-phase perfusive supports (POROS R1/H and POROS R2/H), which have different pore structures, were carried out to obtain the axial dispersion data. The Knox equation and some empirical correlations for dispersion coefficients in porous media were applied to correlate the experimental data. The influences of particle properties, solute molecular sizes and flow velocity on the dispersion coefficient were elucidated. Axial dispersion was recognised to be the main contributor to peak broadening in perfusion chromatography. The dependence of the height equivalent to a theoretical plate on flow-rate was found to be the result of the velocity dependence of the axial dispersion. The dispersion coefficient in a perfusive column can be well represented both by a power–law relationship and a correlation derived based on stochastic theory. Pursuant to these, it was found that pore size distribution of the perfusive particles and solute molecular size are important parameters, which influenced the dispersion results significantly.

Keywords: Axial dispersion; Band spreading; Perfusion chromatography; Proteins

1. Introduction

Axial dispersion in packed beds is known to be a consequence of solute molecular diffusion and velocity distribution within the fluid [1]. An understanding of this is of great practical interest in many industrial processes, such as chromatography and fixed bed reactions. It is therefore not surprising that considerable attention has been placed on its analysis since the early 1970s [2–5]. It has been found that axial dispersion exhibits non-linear velocity dependence. This dependency arises from the coupling that exists between the flow velocity and the boundary layer molecular diffusion in the interstitial pore space [1]. The extent of this velocity dependence is associated with the packing quality of the packed bed.

Axial dispersion in a chromatographic column has been considered in the plate theory of chromatography by several researchers [5–7]. It is widely accepted that the contribution of axial dispersion to column efficiency is insignificant in conventional chromatography compared to the slow mass transfer

*Corresponding author. Tel.: +65-8742-174; fax: +65-7791-936.

E-mail address: chelohkc@nus.edu.sg (K.-C. Loh).

0021-9673/01/$ – see front matter
PII: S0021-9673(01)00725-7

or equilibration rates occurring inside the particles [8,9]. However, a re-analysis has recently come to light. Knox [10] found that at the flow-rates used in modern high-performance liquid chromatography (HPLC), which are near those giving minimum *h* (reduced plate height), the most important contribution to band broadening comes from axial dispersion. Axial dispersion has also been found to be the main contributor to peak spreading in membrane chromatography [11,12].

Perfusion chromatography was introduced in the early 1990s [13]. The packing particles in this case are fabricated from the polymerisation of agglomerated microspheres [13,14]. Using a porosimetry technique in conjunction with network simulations, these particles were reported to have a bimodal pore size distribution, consisting of an interconnected network of macropores (pore diameters of the order of 1000 Å) and micropores (pore diameters of the order of 100 Å) [15]. It is a consequence of the pore size distribution and pore arrangement that gives rise to the desired combination of high capacity, high speed and high-resolution separation of biomolecules in perfusion chromatography.

It has been accepted for a long time that the macropores allow a significant level of forced intraparticle convection [13,16–19]. The enhancement of intraparticle mass transport by this intraparticle forced convective flow in perfusion chromatography has been recognised in numerous past studies, which have included moment analysis [16–18], numerical solution of the full mass transfer equation [19] and discrete network modelling [15,20]. The focus of these studies has been the intraparticle convection enhanced mass transfer behaviour. In these previous studies, axial dispersion coefficient was either neglected or estimated from existing empirical correlations derived from studies of conventional chromatography.

It has been demonstrated that, in perfusion chromatography, the column efficiency and dynamic capacity are not compromised at high flow-rates [13,16]. The height equivalent to a theoretical plate (HETP) curve, under non-retained conditions, reaches a plateau at high flow-rates. This phenomenon has also been observed in the studies of membrane chromatography [11,12]. In the latter, dispersion was found to be the main contributor to peak spreading. Accordingly, in perfusion chromatography, it is anticipated that the main contribution to band broadening might also be the axial dispersion in the column. However, hitherto, the importance and the peculiarity of axial dispersion in perfusion chromatography have not been properly understood.

The aim of this study is to propose an alternative interpretation of band spreading in perfusion chromatography by elucidating the importance of axial dispersion in the column packed with POROS materials. Elution chromatography of proteins under non-retained conditions on two reversed-phase perfusive supports (POROS R1/H and POROS R2/H), which possess different pore structures, was carried out to obtain the axial dispersion data. Bovine serum albumin (BSA) and lysozyme were chosen as the model proteins to represent biomolecules of different sizes. The Knox equation and some correlations for dispersion coefficients in porous media were applied to correlate the experimental data. The effects of particle pore structures, solute molecular sizes and flow velocity on the dispersion coefficient were determined. It is hoped that the findings in this study will further enhance the understanding of the mass transfer behaviour in perfusion chromatography.

2. Experimental

2.1. Apparatus and materials

Chromatographic experiments were carried out on a Waters (Milford, MA, USA) HPLC system equipped with a 600E multisolvent delivery pump, a 717 plus auto-sampler and a 2487 dual-wavelength absorbance detector. The system was operated using the Millenium^{32} Chromatography Manager supplied by Waters.

The chromatographic columns used in our experiments (POROS R1/H and POROS R2/H, 100×4.6 mm, particle diameter d_p=10 μm) were obtained from Perkin-Elmer (Norwalk, CT, USA).

HPLC-grade acetonitrile (ACN) and reagent-grade trifluoroacetic acid (TFA) were obtained from Fisher Scientific (Fair Lawn, NJ, USA). BSA and lysozyme were purchased from Sigma (St. Louis, MO, USA). The molecular masses of BSA and lysozyme are, respectively, 67 000 and 13 930 [21], and the respec-

tive diffusivities, D_m, are $7.50 \cdot 10^{-7}$ and $1.36 \cdot 10^{-6}$ cm^2/s.

2.2. Methods

The HETP data were obtained for each protein (1.0 mg/ml solution) by a series of 10-μl injections using the auto-sampler. The flow-rate of the mobile phase ranged from 1.0 to 10.0 ml/min, the corresponding superficial velocity of which was from 0.05 to 1.0 cm/s. The experiments were conducted at room temperature of 25°C. The 2487 dual-wavelength absorbance detector was set at 280 nm with single channel detection. The ACN concentration (%, v/v) in the eluent of ACN–water+0.1% TFA was 55 and 50% for BSA and lysozyme, respectively. This ensured non-retention of the proteins on the packing media. The densities of the corresponding mobile phases, ρ, were determined as 0.904 and 0.917 g/cm^3, respectively. The corresponding values of viscosity, η, were 0.0079 and 0.0084 g/cm s, respectively.

Prior to the injection, the column was equilibrated with at least 20 column volumes of the mobile phase. The injection at each flow-rate was duplicated at least once. The extra column effects were taken into account by repeating the experiments without the column under the same experimental conditions for each respective sample.

The chromatograms obtained were exported to Microsoft Excel by Millenium[32] for further numerical treatment. The HETP data of the column were obtained by the equation:

$$\mathrm{HETP} = \frac{(\sigma_2^2 - \sigma_1^2)L}{(\mu_2 - \mu_1)^2} \quad (1)$$

where μ_1 and σ_1^2 are, respectively, the first moment and peak variance without the column, while μ_2 and σ_2^2 are, respectively, the total first moment and peak variance with the column on-line and L is the column length. The axial dispersion coefficient, D_{ax}, was obtained from:

$$D_{ax} = \frac{\mathrm{HETP}u_0}{2} \quad (2)$$

where u_0 is the interstitial velocity (u/ϵ), u is the superficial velocity, and ϵ is the bed porosity based on the sum of the interstitial and intraparticle flow-through pores. This was calculated by dividing the average elution volume for each protein by the column volume, since the elution volumes for both proteins were almost constant over the entire range of mobile phase flow-rates investigated (Fig. 1). It is worth noting that the elution volume for lysozyme was higher than that for BSA. This is a clear reflection of size-exclusion effects. Furthermore, the difference between the elution volumes for BSA and lysozyme is larger on POROS R2/H than that on POROS R1/H. It has been reported that, compared with POROS R2/H, POROS R1/H has more tightly agglomerated microspheres, larger agglomerates and hence larger spaces between the agglomerates [14]. The larger difference of elution volumes for BSA and lysozyme on POROS R2/H indicates that size-

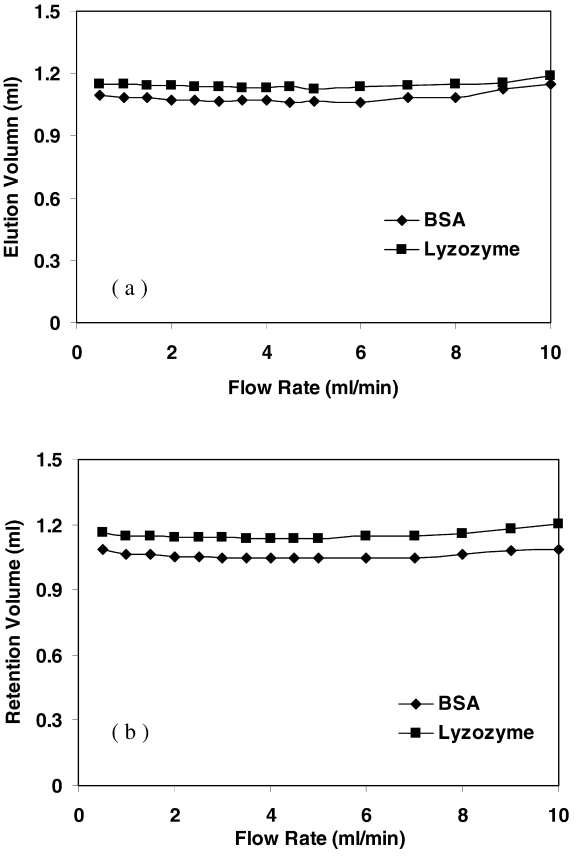

Fig. 1. Column elution volume for proteins. (a) POROS R1/H; (b) POROS R2/H.

exclusion effects are different on these two kinds of materials due to their different pore size distributions. Subsequently, we will show that size-exclusion effects also play a role in the dispersion data.

3. Results and discussion

3.1. HETP results and the Knox equation

Assuming a power–law velocity dependency for the axial dispersion, Bristow and Knox [5] obtained the following equation for liquid chromatography (subsequently referred to as the Knox equation):

$$h = Av^{1/3} + \frac{B}{v} + Cv \quad (3)$$

where h is the reduced plate height (HETP/d_p), v is reduced mobile phase velocity (ud_p/D_m), u is superficial velocity, d_p is particle diameter, and D_m is molecular diffusivity of the solute. Another widely accepted equation for describing the dependence of the plate height on mobile phase linear velocity is the van Deemter equation [6]:

$$h = A + \frac{B}{v} + Cv \quad (4)$$

The above two equations are the two most commonly encountered equations in the plate theory of chromatography. The only difference between them lies in the velocity dependency of the first term. This term represents the broadening that results from radial velocity inhomogeneity-induced axial dispersion and from resistance to mass transfer in the moving phase. The second term arises from the axial molecular diffusion, which is inversely proportional to velocity. The third term represents the slowness of equilibration or mass transfer in the stationary phase. The Knox equation provides better fits to liquid chromatography data than the van Deemter equation due to the simultaneous contribution of convection and radial diffusion in the interstitial void space of the packing [4,7,10]. The magnitude of the A value is indicative of the packing quality of the bed [4,10], which is a consequence of the velocity distribution within the pore spaces.

Under the conditions in which we conducted the experiments, the B term in the Knox equation is negligible and therefore the Knox equation reduces to:

$$h = Av^{1/3} + Cv \quad (5)$$

Fig. 2 shows the calculated reduced plate height (using the Knox equation) and the experimental results for each protein on two different POROS R1/H and POROS R2/H columns, respectively. As can be seen, the dispersion data corroborated reasonably well the Knox equation over the whole range of fluid velocity investigated. The fitting parameters are summarised in Table 1. For both BSA and lysozyme, on both columns of POROS R1/H and of POROS R2/H, all the A values were found to be non-zero, although the C values were almost negligible. This suggests that, for the case of perfusion chromatography, axial dispersion arising from the non-uniform velocity distribution over the column cross-section is indeed the main contributor to column efficiency. This is similar to Knox's recent report [10] that at the flow-rates of modern HPLC, which are near those giving minimum h, the most important contribution to band broadening of conventional LC column comes from axial dispersion. However, in the case of perfusion chromatography, axial dispersion seems to control the band spreading over a much wider range of flow-rates. The insignificance of the C term may be due to the size-exclusion effect of the protein molecules, which have been denied access to most of the micropores (pores inside the agglomerates of microspheres). Based on this analysis, the observed flattening of the HETP with velocity increase in perfusion chromatography is, in fact, the result of axial dispersion dependency on velocity. This velocity dependence can be attributed to the combination of the multiple path flow and the boundary layer molecular diffusion within the flow-through pores inside the perfusive columns. The flattening of HETP was gradual, rather than steep as on other materials [22,23]. This gentler dependence of HETP upon velocity may be ascribed to the specific pore structures of the POROS materials, i.e., the wider pore size distributions. In this case, the competition between the multiple path flow and the boundary layer molecular diffusion might be gradual with increasing velocity.

In addition to an excellent fit of the h–v data by

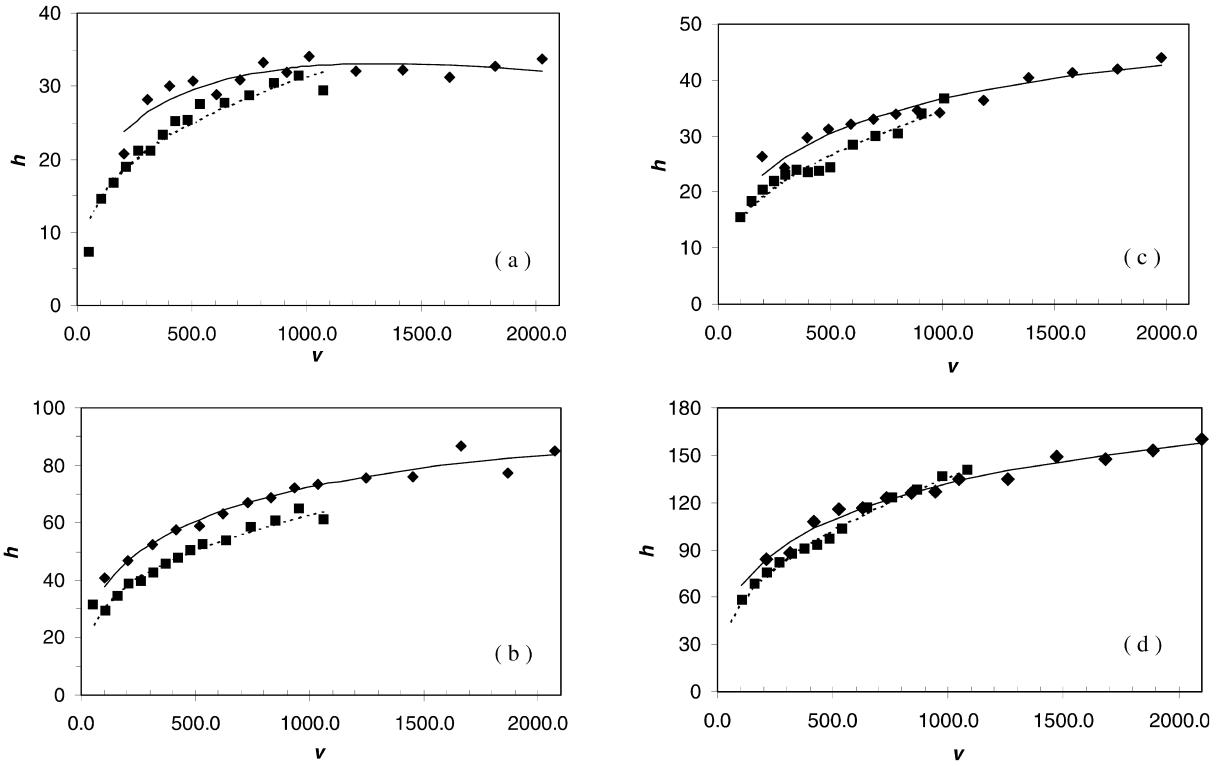

Fig. 2. Reduced HETP as a function of reduced fluid velocity for proteins (BSA ♦ and lysozyme ■). The curves are correlation results using the Knox equation. (a) POROS R1/H (2862); (b) POROS R2/H (1929); (c) POROS R1/H (2457); (d) POROS R2/H (1931).

the Knox equation, the magnitude of the fitting parameters are even more interesting. The *A* value provides a measure of the packing quality of the column and therefore the reproducibility is anticipated to be column dependent. This is evidenced by the different *A* values obtained from the experiments performed on the two different columns for each kind of packing material (Table 1). The larger the deviation of the value from unity, the poorer is the packing quality [10]. The values obtained from our model fits are consistent with these obtained by Knox and Scott [24] for columns packed with 50 μm ODS silica gel, albeit higher in our case. These large *A* values can be attributed to the velocity hetero-

Table 1
Fitting parameters for the Knox equation

Solute	POROS R1/H (2862)		POROS R2/H (1929)	
	A	*C*	*A*	*C*
BSA	3.9	0.01	7.2	0.01
Lysozyme	2.9	0.00	6.1	0.00
	POROS R1/H (2457)		POROS R2/H (1931)	
	A	*C*	*A*	*C*
BSA	4.1	0.001	15	0.01
Lysozyme	3.2	0.003	12	0.02

geneity caused by the intraparticle convection [13,16–19]. This is even more significant for the case of POROS R2/H, as a result of the smaller sizes of the so-called intraparticle flow-through pores [14,15]. With respect to the convective flow in the interstitial space, as well as in the intraparticle flow-through pores, the perfusive column can therefore be visualised as being packed with the agglomerates of microspheres in the perfusive particles. Based on this representation, it is therefore not surprising that the packing quality of the bed is very ''poor''. A schematic of this visualization is found in Fig. 3. Note that the *A* values for lysozyme were smaller than those for BSA in both of the columns. This indicates that the heterogeneities of the pore space diminish with respect to smaller molecules, an indication of size-exclusion effects. In comparing between the two types of packing, POROS R2/H has larger *A* values, suggesting that the ''packing quality'' of the POROS R2/H column was also worse than that of POROS R1/H. These observations clearly demonstrate that, in perfusive columns, the extent of the velocity dependency of the *A* term varies with the pore size distributions of the perfusive particles, as well as the solute molecular sizes.

3.2. Axial dispersion correlation

In order to further reinforce the contribution of axial dispersion to band spreading in perfusion chromatography, in the following, the Gunn's correlation for axial dispersion in a packed bed was used to correlate the experimental dispersion data. Based on a stochastic analysis, Gunn [2,3] has shown that:

$$\frac{1}{\mathrm{Pe}} = \frac{D_{\mathrm{ax}}}{ud_{\mathrm{p}}} = \left\{ \frac{\mathrm{ReSc}}{\epsilon\Gamma} \cdot (1-p)^2 + \frac{\mathrm{Re}^2\mathrm{Sc}^2}{\epsilon^2\Gamma^2} \cdot p(1-p)^3 \times \left[\exp\left(\frac{-\epsilon\Gamma}{p(1-p)\mathrm{ReSc}} \right) - 1 \right] \right\} \cdot (1+\sigma_{\mathrm{v}}^2) + \frac{\sigma_{\mathrm{v}}^2}{2} + \frac{\epsilon}{\tau\mathrm{ReSc}} \quad (6)$$

Here, Pe ($u_0 d_{\mathrm{p}}/D_{\mathrm{ax}}$) is the Peclet number, Re ($\rho u d_{\mathrm{p}}/\eta$) is the Reynolds number, Sc ($\eta/\rho D_{\mathrm{m}}$) is the Schmidt number, α_1 is the first zero of the Bessel function, $J_0(x)$ (which is equal to 2.4048), Γ is a characteristic of the packed bed given as $4(1-\epsilon)\alpha_1^2/\epsilon$, p is the probability of axial displacement [which is a function of Reynolds number, defined, for spheres, as $p = 0.17 + 0.33\exp(-24/(\epsilon\mathrm{Re}))$], and τ is the tortuosity factor (ca. 1.4 for spheres). It is noteworthy that, after some algebraic manipulations, Eq. (6) is equivalent to an HETP equation for a column that is purely axial dispersion controlled.

In Eq. (6), σ_{v}^2 is the variance of velocity distribution over the cross-section of the column, and is a measure of the packing quality in the column. The better the bed packing quality, the lower will be the value of σ_{v}^2 [3].

The experimental axial dispersion coefficient was obtained directly from Eq. (2) and a least-squares fit to Eq. (6) was performed using 0.6 μm and 0.31 μm as the mean particle diameters for POROS R1/H and POROS R2/H [14], to determine the Reynolds number. The correlation results are shown in Fig. 4. It can be seen that the agreement between experimental and simulated data is very good.

The resulting σ_{v}^2 values are listed in Table 2. The typical value of σ_{v}^2 for a well-packed bed was reported to be 0.1–0.3 for particles 0.37 to 6.0 mm [3]. Although no direct σ_{v}^2 values for a conventional LC column have been reported in the literature, it is anticipated that this value will be higher than 0.1–0.3 due to the much smaller sizes of the packing particles in a liquid chromatographic column. It has

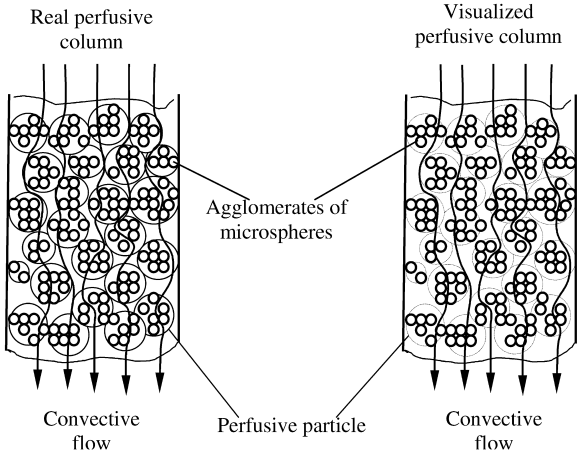

Fig. 3. Visualisation of a perfusive column as a ''poorly'' packed bed.

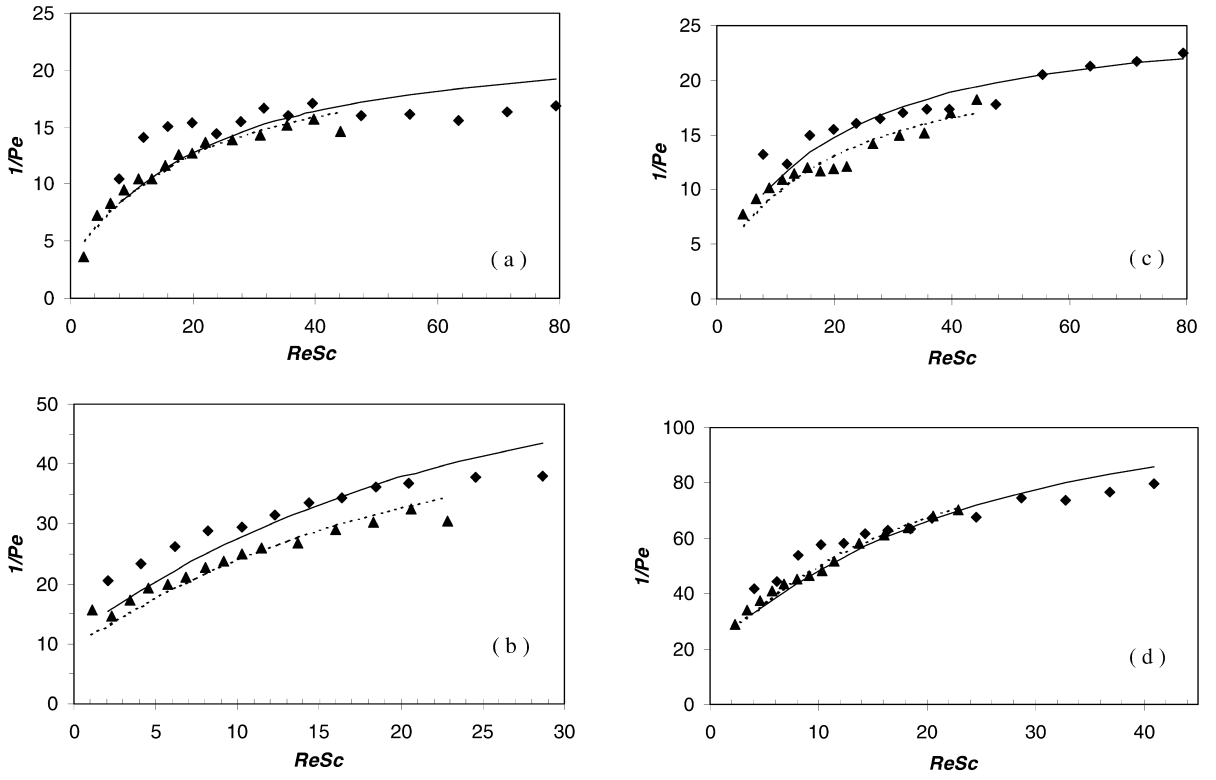

Fig. 4. Gunn's equation fitting results for proteins on (a) POROS R1/H (2862); (b) POROS R2/H (1929); (c) POROS R1/H (2457); (d) POROS R2/H (1931). The solid points are the experimental results for proteins (BSA ♦, lysozyme ■). The solid lines are the Gunn's equation predictions for BSA, while the dashed lines are those for lysozyme.

also been reported that for particles ranging in size down to 50 μm, values of σ_v^2 were as large as 2.0 for experiments at low Reynolds numbers [3]. By performing a similar correlation of the h–v data found in the literature [25,26] with Eq. (6), we obtained σ_v^2 of 0.8–0.9 for the Zorbax columns packed with 5 μm and 10 μm diffusive spherical silica particles. Notwithstanding, the σ_v^2 values obtained for perfusive columns are much higher, indicating the significant maldistribution of the fluid velocity over the column cross-section. This again can be ascribed to the pore space heterogeneities caused by the big differences between the sizes of the interstitial and the intraparticle flow-through pores. In addition, σ_v^2 values were larger for BSA than for lysozyme on both kinds of the columns, which seem to imply that the velocity distribution for the mobile phase carrying lysozyme is relatively less heterogeneous due to the smaller solute size. This could possibly be due to the fact that smaller molecules are able to sample more pore spaces, resulting in a less heterogeneous solute velocity distribution. Furthermore, σ_v^2 values for POROS R2/H were also larger than that for POROS R1/H, suggesting that a more heterogeneous velocity distribution exists on POROS R2/H. These results are totally consistent with the analysis by the Knox equation and the reported characterisation studies of the perfusive media [14,15].

Table 2
σ_v^2 values in Eq. (6)

	POROS R1/H		POROS R2/H	
Column serial No.:	2862	2457	1929	1931
BSA	7.0	8.1	23	41
Lysozyme	6.6	6.9	18	38

Besides using the Gunn's correlation, experimental dispersion data in porous media are most fre-

quently presented in the form of D_{ax}/D_m versus Pe_b diagrams, where D_{ax} is the observed axial dispersion coefficient and Pe_b is the bed Peclet number. Fried and Combarnous [27] showed that there are five different regimes of dispersion in flow-through porous media. They are the diffusion regime, transition regime, power–law regime, pure convection regime and turbulent dispersion regime. From our analysis by the Knox and the Gunn's equations, the dispersion data from the perfusive beds may lie within the power–law regime, in which the axial dispersion is expressed as [28]:

$$\frac{D_{ax}}{D_m} = \alpha \cdot Pe_b^{\beta} \quad (7)$$

where α and β are constants. The above equation is valid for Peclet numbers between 5 and 10 000. The value of α depends on the heterogeneities of the pore space. The typical value for α is 0.5 and the average value for β is about 1.2. Sahimi [28] also mentioned that this value for β is not universal, usually depending on the shapes of the pores. In the power–law regime, convection dominates dispersion, but the effect of diffusion within the boundary layer near the solid surface inside the pore space cannot be neglected.

Fig. 5 displays the experimental and the power–law predicted results of the dispersion data in the POROS R1/H and R2/H perfusive beds. The fitting values of α and β are listed in Table 3. It can be seen that the reproducibility of these values for both the columns of POROS R1/H and of POROS R2/H is rather good. Compared with the typical value of 0.5, the α values obtained were much larger. Although no α values for LC columns were directly available in the literature, the very big difference between the obtained values and the typical value of 0.5 suggests that the pore space over the perfusive column cross-section is significantly heterogeneous. POROS R2/H is more heterogeneous than POROS R1/H, resulting in larger α values. Moreover, for lysozyme, this heterogeneity is less strongly manifested due to its smaller molecular size. The above results are in very good agreement with those obtained from the analysis by Eqs. (5) and (6). On the other hand, it can also be found that β values did not deviate much from its typical value of 1.20 very much, albeit slightly higher in some cases. This is consistent with that reported by Colin et al. [29], that the pore size distribution and pore interconnectivity in the particles are more important parameters than the pore shapes to determine dispersion in the flow-through porous media.

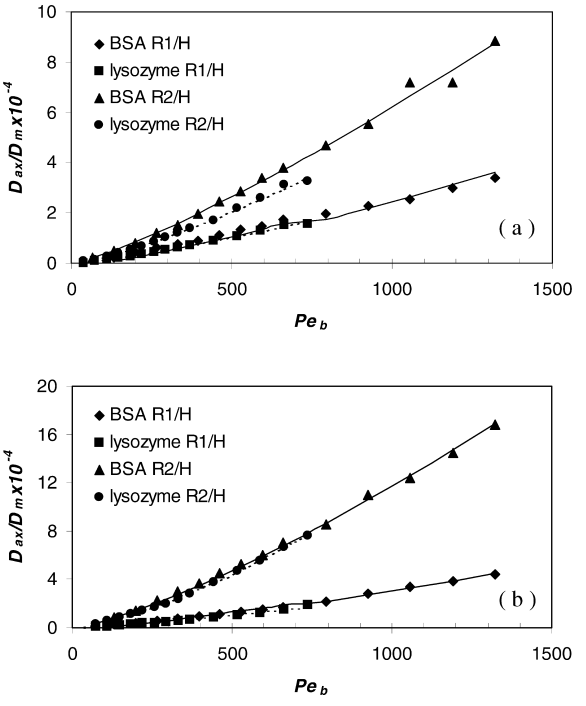

Fig. 5. Dependence of axial dispersion coefficient on the bed Peclet number. (a) POROS R1/H (2862) and R2/H (1929); (b) POROS R1/H (2457) and R2/H (1931). The solid points are the experimental results and the solid (BSA) and dashed (lysozyme) lines are the simulations by the power–law relationship.

Analyses by the above correlations lead us to conclude that axial dispersion is the major contributor to peak spreading in perfusion chromatography. It has a much stronger velocity dependency than that in a conventional packed bed. This is possibly due to the large differences between the sizes of the interstitial and intraparticle flow-through pores. Since the velocity dependency of axial dispersion arises from the combined effects of the multiple path flow and molecular diffusion within the boundary layer of the pore spaces [1,28], we could conclude that, for the case of a perfusive bed, in

Table 3
Fitting parameters for Eq. (7)

Solute	POROS R1/H (2862)		POROS R2/H (1929)	
	α	β	α	β
BSA	6.0	1.2	12	1.2
Lysozyme	4.5	1.2	6.0	1.3
	POROS R1/H (2457)		POROS R2/H (1931)	
	α	β	α	β
BSA	7.1	1.2	13	1.3
Lysozyme	4.5	1.3	6.4	1.4

which the sizes of the intraparticle flow-through pores are of the order of 1000's Å [14,15], the boundary layer effects may be more significant.

4. Conclusions

A series of model simulations lead us to the conclusion that when separating large biomolecules, axial dispersion arising from the non-homogeneous flow within the interstitial and intraparticle flow-through pores presents the main contribution to peak spreading in perfusion chromatography. The observed flattening of HETP in perfusion chromatography is, in fact, a result of the velocity dependence of the axial dispersion. Moreover, the extent of this velocity dependency is much stronger than in a conventional diffusive packed bed, and it varies with the pore size distributions of the perfusive particles as well as the solute molecular sizes. The larger the difference between the pore sizes, the stronger the velocity dependency of the axial dispersion; the smaller the solute molecular size, the less significant is the velocity dependency. Compared to the effects of pore size distribution, the extent of the velocity dependency is less affected by the effect of different pore shapes.

5. Nomenclature

A	A term in the Knox equation
B	B term in the Knox equation
C	C term in the Knox equation
d_p	Particle diameter (cm)
D_{ax}	Axial dispersion coefficient (cm^2/s)
h	Reduced plate height, $HETP/d_p$
$J_0(x)$	Bessel function of first kind, zeroth order
L	Column length
p	Probability of axial displacement
Pe	Peclet number ($u_0 d_p/D_{ax}$)
Pe_b	Bed Peclet number (ud_p/D_m)
R^2	Correlation coefficient
Re	Reynolds number based on particle diameter and superficial velocity, $\rho u d_p/\eta$
Sc	Schmidt number, $\eta/\rho D_m$
u	Superficial velocity (cm/s)
u_0	Interstitial velocity (cm/s)
v	Reduced mobile phase velocity (ud_p/D_m)
α	Correlation parameter for the dispersion coefficient in Eq. (7)
α_1	First zero of equation $J_0(x)=0$
β	Correlation parameter for the dispersion coefficient in Eq. (7)
ϵ	Bed porosity
Γ	The characteristic of the packed bed, $(1-\epsilon)\alpha_1^2/\epsilon$
η	Mobile phase viscosity (g/cm s)
μ_i	First moment (s, $i=1, 2$)
ρ	Mobile phase density (g/cm^3)
σ_i^2	Peak variance (s^2, $i=1, 2$)
σ_v^2	Variance of velocity distribution over the cross section of a column
τ	Tortuosity factor

Acknowledgements

The authors wish to acknowledge the graduate scholarship to A. Geng provided by The National University of Singapore.

References

[1] G. Guiochon, S.G. Shirazi, A.M. Katti, Fundamentals of Preparative and Nonlinear Chromatography, Academic Press, Boston, MA, 1994.
[2] D.J. Gunn, Trans. Inst. Chem. Eng. 47 (1969) 351.
[3] D.J. Gunn, Chem. Eng. 49 (1971) 109.
[4] J.H. Knox, J.F. Parcher, Anal. Chem. 41 (1969) 1599.
[5] P.A. Bristow, J.H. Knox, Chromatographia 10 (1977) 279.
[6] J. van Deemter, F. Zuiderweg, A. Klinkenber, Chem. Eng. Sci. 5 (1956) 271.
[7] J.C. Giddings, Dynamics of Chromatography – Part 1: Principles and Theory, Marcel Dekker, New York, London, 1965.
[8] F.H. Arnold, H.W. Blanch, C.R. Wilke, Chem. Eng. J. 30 (1985) B25.
[9] F.H. Arnold, H.W. Blanch, C.R. Wilke, Chem. Eng. J. 30 (1985) B9.
[10] J.H. Knox, J. Chromatogr. A 831 (1999) 3.
[11] D.D. Frey, R.V. Water, B.B. Zhang, J. Chromatogr. 603 (1992) 43.
[12] A. Shiosaki, M. Goto, T. Hirose, J. Chromatogr. A 679 (1994) 1.
[13] N.B. Afeyan, S.P. Fulton, N.F. Gordon, L. Mazaroff, L. Varady, F.E. Regnier, Bio/Technology 8 (1990) 203.
[14] D. Whitney, M. McCoy, N. Gordon, N. Afeyan, J. Chromatogr. A 807 (1998) 165.
[15] K.C. Loh, D.I.C. Wang, J. Chromatogr. A 718 (1995) 239.
[16] A.E. Rodrigues, Z.P. Lu, J.M. Loureiro, Chem. Eng. Sci. 46 (1991) 2765.
[17] D.D. Frey, E. Schweinheim, Cs. Horváth, Biotechnol. Prog. 9 (1993) 273.
[18] G. Carta, A.E. Rodrigues, Chem. Eng. Sci. 48 (1993) 3927.
[19] A.I. Liapis, M.A. McCoy, J. Chromatogr. 599 (1992) 87.
[20] J.J. Meyers, A.I. Liapis, J. Chromatogr. A 827 (1998) 197.
[21] H.A. Sorber (Ed.), Handbook of Biochemistry, Selected Data for Molecular Biology, CRC Press, Cleveland, OH, 1970.
[22] A.E. Rodrigues, J.M. Loureiro, C. Chenou, M. Rendueles de la Vega, J. Chromatogr. B 664 (1995) 233.
[23] S. Yamamoto, E. Miyagawa, J. Chromatogr. A 852 (1999) 25.
[24] J.H. Knox, H.P. Scott, J. Chromatogr. 282 (1983) 197.
[25] T. Farkas, M.J. Sepaniak, G. Guiochon, J. Chromatogr. A 740 (1996) 169.
[26] T. Farkas, G. Guiochon, Anal. Chem. 69 (1997) 4592.
[27] J.J. Fried, M.A. Combarnous, Adv. Hydrosci. 7 (1971) 169.
[28] M. Sahimi, Flow and Transport in Porous Media and Fractured Rock: From Classical Methods to Modern Approaches, VCH, Weinheim, 1995.
[29] H. Colin, J.C. Diez-Masa, T. Czaychowska, I. Miedziak, G. Guiochon, J. Chromatogr. 167 (1978) 41.